



HAL
open science

Straightforward synthesis of ferrocenyl allylic thioethers

Rafika Bouchene, Jean-Claude Daran, Rinaldo Poli, Éric Deydier, Sofiane Bouacida, E. Manoury

► **To cite this version:**

Rafika Bouchene, Jean-Claude Daran, Rinaldo Poli, Éric Deydier, Sofiane Bouacida, et al.. Straightforward synthesis of ferrocenyl allylic thioethers. *Inorganica Chimica Acta*, 2018, 470, pp.365-372. 10.1016/j.ica.2017.06.039 . hal-01954089

HAL Id: hal-01954089

<https://hal.science/hal-01954089>

Submitted on 1 Mar 2021

HAL is a multi-disciplinary open access archive for the deposit and dissemination of scientific research documents, whether they are published or not. The documents may come from teaching and research institutions in France or abroad, or from public or private research centers.

L'archive ouverte pluridisciplinaire **HAL**, est destinée au dépôt et à la diffusion de documents scientifiques de niveau recherche, publiés ou non, émanant des établissements d'enseignement et de recherche français ou étrangers, des laboratoires publics ou privés.

Straightforward synthesis of ferrocenyl allylic thioethers.

Rafika Bouchene,^{a,b,c,d} Jean-Claude Daran,^{a,b} Rinaldo Poli,^{a,b,e} Eric Deydier,*^{a,b,f}
Sofiane Bouacida,^{c,d} Eric Manoury*^{a,b}

^aCNRS, LCC (Laboratoire de Chimie de Coordination), 205 route de Narbonne, BP 44099, F-31077 Toulouse Cedex 4, France CNRS. Fax: +33-561553003; Tel: +33-561333174; E-mails: eric.deydier@iut-tlse3.fr; eric.manoury@lcc-toulouse.fr.

^bUniversité de Toulouse, UPS, INPT, F-31077 Toulouse Cedex 4, France

^cDépartement Sciences de la Matière, Faculté des Sciences Exactes, Université Oum El Bouaghi, 04000, Algeria

^d Unité de Recherche de Chimie Moléculaire et Structurale CHEMS, Université Mentouri, Constantine, Algeria.

^e Institut Universitaire de France, 1, rue Descartes, 75231 Paris Cedex 05, France.

^f IUT A Paul Sabatier, Département de Chimie, Avenue Georges Pompidou, CS 20258, F-81104 Castres Cedex, France

Abstract

The new ferrocenyl allylic thioethers FcCH=CHCH₂SR (**2a-e**) and FcCH(SR)CH=CH₂ (**3a-e**) (R = Ph, **a**; 2-naphthyl, **b**; 3,5-C₆H₃Me₂, **c**; *i*Pr, **d**; *t*Bu, **e**) were synthesized in good yields from the ferrocenyallylammonium salt [**1**]⁺I⁻ and the corresponding thiol RSH. With sufficiently strong bases to fully deprotonate the thiol, good to excellent regioselectivities (88-99%) in favor of the linear isomer **2** were obtained. The molecular structures of **2a** and **2b** were obtained by X-ray diffraction on monocrystals. A mechanistic proposal based on experimental data and supported by calculations is also presented, underlying the role of the base in the reaction regioselectivity.

Keywords: ferrocene; thiols; allylic thioethers; nucleophilic substitution; regioselectivity; DFT calculations.

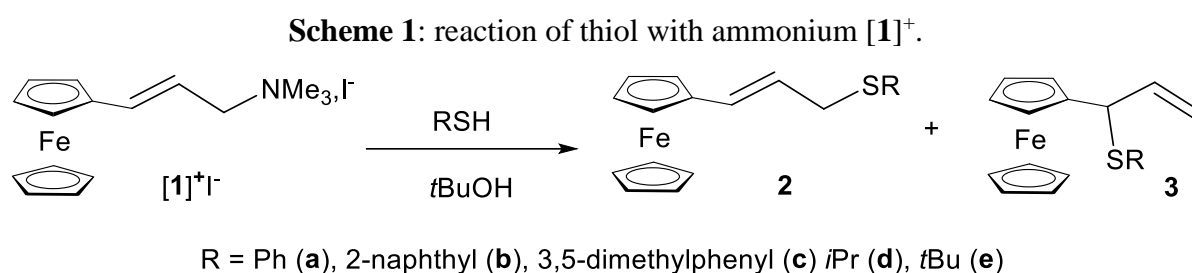
This article is dedicated to Pr Carlo Mealli.

1. Introduction

In the last decades, many efforts have been devoted to the synthesis of allyl thioethers,^{1,2,3,4,5,6,7,8,9,10,11,12, 13} because these compounds may have interesting properties in many areas such as biochemistry and medicinal chemistry,^{14,15} materials science¹⁶ or synthetic organic chemistry as synthetic intermediates.^{17,18,19,20,21,22} Despite the huge interest for ferrocene derivatives in many areas such as catalysis,^{23,24,25,26,27,28,29,30} supramolecular chemistry^{31,32} and sensing, and medicinal chemistry,^{33,34} no ferrocene-containing allyl thioethers have been described so far to the best of our knowledge. In this article, we wish to present the synthesis of the first members of this thioether family.

2. Results and discussion

We have recently described a new and efficient synthesis of ferrocenylamines starting from the ferrocenylammonium salt **[1]⁺I⁻**.³⁵ In this contribution we present the reaction between **[1]⁺I⁻** and thiol nucleophiles (see scheme 1).

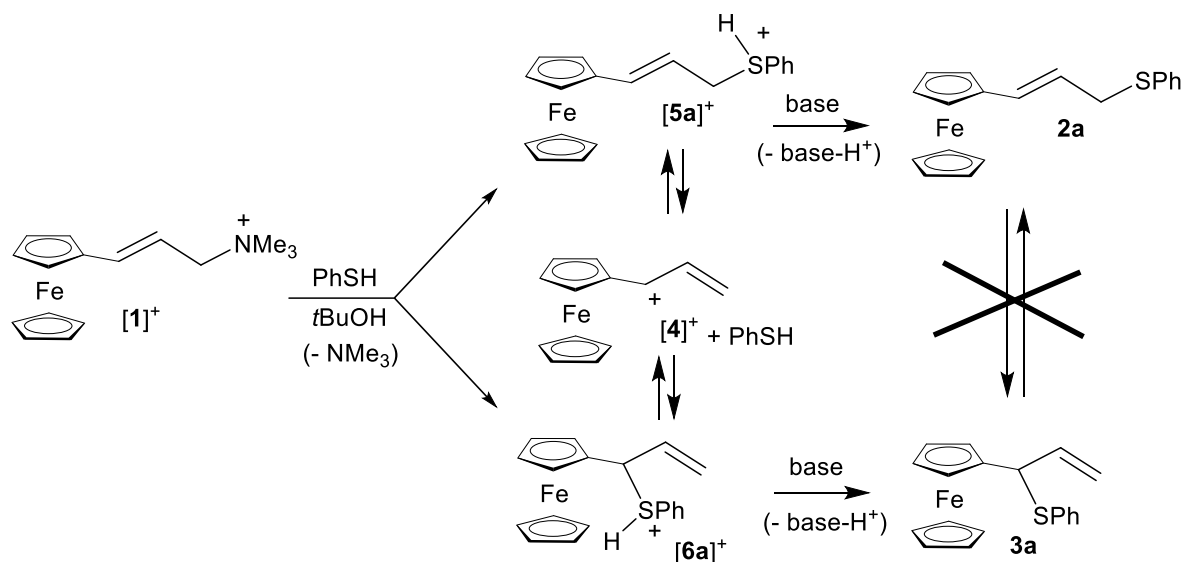


The reactions were carried out in *tert*-butanol at 90°C. Under these conditions with thiophenol as nucleophile, the **[1]⁺I⁻** conversion was complete in 16 h to yield the desired ferrocenyl allyl thioethers in good yields as a mixture of the two regioisomers **2a** and **3a** in nearly equimolar amounts (Scheme 1; Table 1, entry 1). This observed regioselectivity may result either from the selectivity of the thiol attack on the ammonium cation **[1]⁺** or from a rearrangement of the sulfonium intermediates **[5a]⁺** and **[6a]⁺** via a carbocation intermediate before deprotonation (see Scheme 2), as proposed for similar reactions of **[1]⁺** with amines as

nucleophiles.³⁵ We suppose that, once formed, the products are stable with respect to isomerization in the presence of ammonium cations.

Since sulfoniums are very strong acids,^{36,37,38,39} we presume that they may be very efficiently deprotonated by the trimethylamine concomitantly produced in the nucleophilic substitution (Scheme 2, base = NMe₃), which would then prevent the interconversion at the level of the sulfonium intermediates. However, it is not possible to completely rule out the possibility of a very fast equilibration between the sulfonium cations. Therefore, we have repeated the reaction in the presence of an external base to potentially accelerate the sulfonium deprotonation.

Scheme 2: Possible pathways leading to the **2a/3a** product distribution.



When potassium carbonate was added to the reaction mixture, the regioselectivity was almost completely shifted in favor of the linear regioisomer **2a**. Carbonate is actually sufficiently basic to deprotonate thiophenol (the pK_a values of PhSH and HCO₃⁻ in water are 6.5 and 10.3, respectively)⁴⁰ to produce PhS⁻. Hence, the nature of the nucleophile attacking the starting compound **[1]⁺** has changed. We propose that under these conditions the nucleophilic substitution rather occurs by a S_N2-type reaction with a regioselectivity in favor of the linear isomer **2a** because the carbon atom in the α position relative to the N atom is more electrophilic than the γ -C atom.⁴¹

In the presence of sodium carbonate, excellent regioselectivities in favor of the linear regioisomers **2b** and **2c** were also obtained using other arylthiols as nucleophiles (see table 1,

entries 3 and 4), whereas the regioselectivities were much lower for the reactions with alkylthiols (see table 1, entries 5 and 7). In fact, sodium carbonate is not sufficiently basic to fully deprotonate isopropylthiol ($pK_a = 10.86$)⁴⁰ and *tert*-butylthiol ($pK_a = 11.06$).⁴⁰ It was therefore decided to use a stronger base, strong enough to fully deprotonate these thiols, namely potassium *tert*-butylate, *t*BuOK (pK_a of *t*BuOH = 16.9)⁴². Indeed, this base led to higher regioselectivities in favor of the linear isomers **3d** and **3e** (table 1, entries 6 and 8).

Table 1. Reactions of RSH with [1]⁺I⁻. ^a

Entry	R	Base	2:3/% ^b	Yield (2, 3)/% ^c
1	Ph	-	55:45	48, 22
2	Ph	Na ₂ CO ₃ ^d	99:1	72, 0
3	2-Naphthyl	Na ₂ CO ₃ ^d	98:2	85, 0
4	3,5-C ₆ H ₃ Me ₂	Na ₂ CO ₃ ^d	99:1	66, 0
5	<i>i</i> Pr	Na ₂ CO ₃ ^d	42:58	36, 50
6	<i>i</i> Pr	<i>t</i> BuOK ^e	93:7	89, 4
7	<i>t</i> Bu	Na ₂ CO ₃ ^d	46:54	42, 52
8	<i>t</i> Bu	<i>t</i> BuOK ^e	83:17	73, 14

^a Conditions: [1]⁺I⁻/RSH = 1:2, in *t*BuOH, 90°C, 16 h. ^b Determined by ¹H NMR of the crude product mixture. ^c Isolated after chromatographic separation (see Experimental details). ^d Na₂CO₃/[1]⁺I⁻ = 20. ^e [1]⁺I⁻/RSH = 1:3, *t*BuOK/[1]⁺I⁻ = 2.

2.3 Crystallographic studies.

Single crystals of compounds **2a** and **2b**, suitable for X-ray diffraction analysis, were obtained by slow diffusion of hexane in dichloromethane solutions. Both compounds present closely related structures based on a ferrocene moiety, with one of the two cyclopentadienyl rings substituted by an allyl thioether chain as shown in Figures 1 and 2. The structure of compound **2a** features two crystallographically independent molecules A and B within the asymmetric unit. A molecular fitting⁴³ (Figure 3) reveals that these are well superimposed and their bond lengths and angles (selected values are compared in Table 2) are roughly identical.

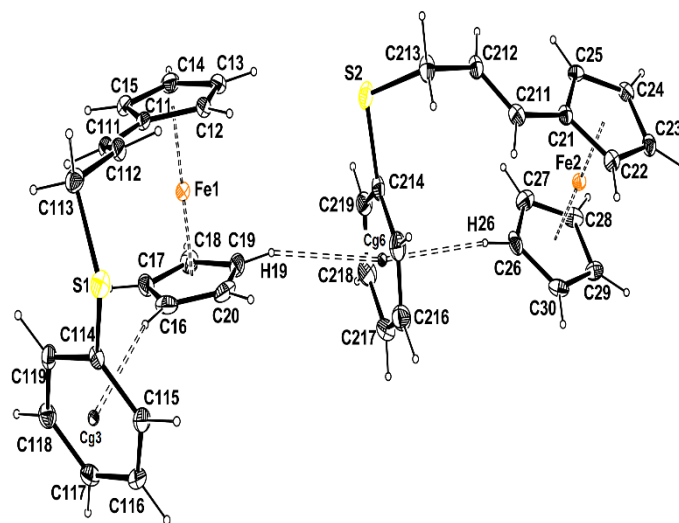


Figure 1. Molecular view of compound **2a** with the atom labelling scheme. Ellipsoids are drawn at the 50% probability level. H atoms are represented as small circle of arbitrary radii. The two molecules A and B building the asymmetric unit are represented for the sake of clarity.

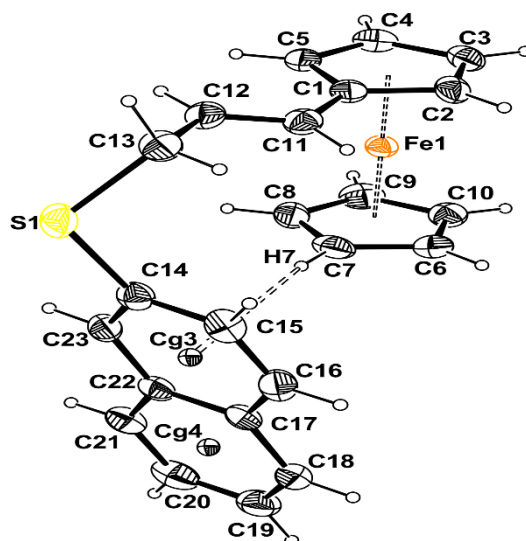


Figure 2. Molecular view of compound **2b** with the atom labelling scheme. Ellipsoids are drawn at the 50% probability level. H atoms are represented as small circle of arbitrary radii.

The Cp rings are nearly eclipsed in both compounds with twist angles τ of $1.40(38)^\circ$, $0.89(40)^\circ$ and $0.95(16)^\circ$ for **2a**(A), **2a**(B) and **2b** respectively. The most interesting feature is the occurrence of C-H \cdots π interactions between one of the CH groups of the unsubstituted Cp ring

and the centroid of the phenyl ring directly attached to the sulfur atom within the same molecule in both **2a(A)** (C16-H16...Cg3) and **2a(B)** (C26-H26...Cg6), as well as across the two different molecules **2a(A)** and **2a(B)** (C19-H19...Cg6) (Table 3, Figure 1). In **2b**, in addition to the same type of CH(Cp)...Ph interaction, there is also a CH... π interaction between one methylene CH group (C13H13A) and the symmetry-related C17-C22 phenyl ring (see table 3).

Table 2. Selected bond lengths (Å) and angles (°) for the structures of **2a** and **2b**

	2a(A)	2a(B)	2b
Fe(1)-Cg(1)	1.648(3)	1.645(2)	1.651(2)
Fe(1)-Cg(2)	1.653(3)	1.645(2)	1.651(2)
S(1)-C(14)	1.774(2)	1.769(3)	1.777(2)
S(1)-C(13)	1.821(3)	1.825(3)	1.839(2)
C(1)-C(11)	1.461(3)	1.453(3)	1.463(3)
C(11)-C(12)	1.326(4)	1.326(4)	1.325(3)
C(12)-C(13)	1.490(3)	1.489(3)	1.490(3)
Cg(1)-Fe(1)-Cg(2)	179.16(12)	179.33(30)	178.05
C(2)-C(1)-C(11)	128.3(2)	128.6(2)	123.49(18)
C(5)-C(1)-C(11)	124.8(2)	124.5(2)	129.67(18)
C(12)-C(11)-C(1)	126.8(2)	126.8(2)	126.5(2)
C(11)-C(12)-C(13)	124.0(2)	122.3(3)	122.8(2)
C(12)-C(13)-S(1)	112.72(17)	113.65(17)	113.27(15)
C(14)-S(1)-C(13)	103.76(12)	104.20(12)	101.44(9)

Table 3. Relevant C-H...Cg π interactions in the structures of compounds **2a** and **2b**

Compound 2a				
D-H...A	D-H(Å)	H...A(Å)	D...A (Å)	D-H...A (°)
C16-H16...Cg3	0.95	2.75	3.677(4)	167.0(2)
C26-H26...Cg6	0.95	2.84	3.776(4)	167.5(2)
C19-H19...Cg6	0.95	2.93	3.846(5)	162.0(2)

symmetry code: (i) $-1/4+x, 5/4-y, 3/4+z$

Cg3 is the centroid of the C114-C119 phenyl ring; Cg6 is the centroid for the C214-C219 phenyl ring.

Compound 2b				
D-H...A	D-H(Å)	H...A(Å)	D...A (Å)	D-H...A (°)
C7-H7...Cg3	0.95	2.98	3.914(2)	168.9(1)
C13-H13A...Cg4 ⁱ	0.95	2.83	3.613(2)	138

symmetry code: (i) -x, 1/2+y, 3/2-z

Cg3 is the centroid for the C14-C15-C16-C17-C22-C23 phenyl ring; Cg4 is the centroid of the C17-C22 phenyl ring.

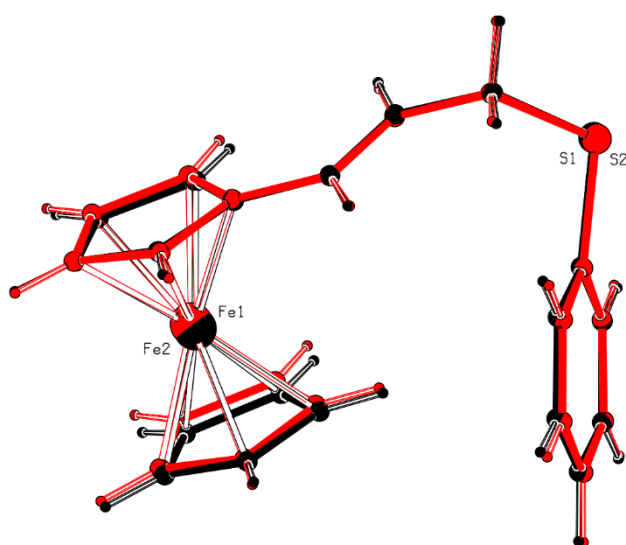
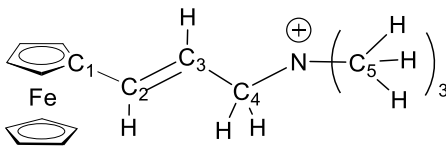


Figure 3. Molecular fitting showing the superimposed molecules (red and black) for **2a**. All atoms are represented as circle.

2.3 Calculations

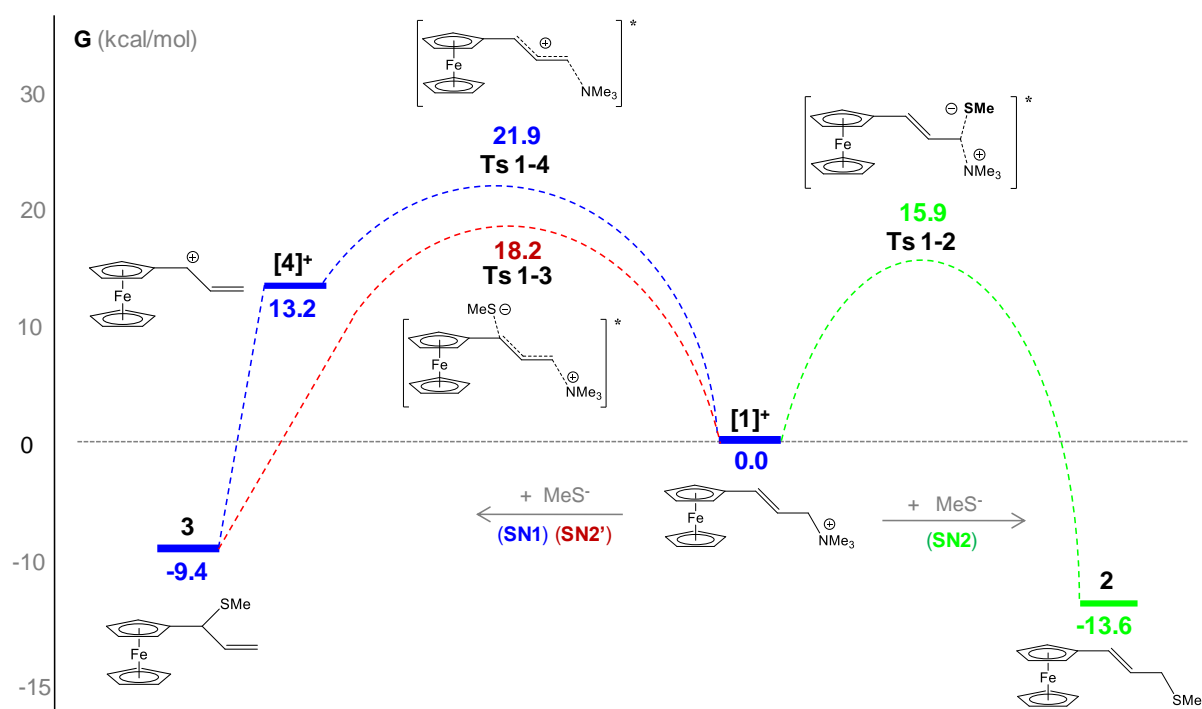
For a better understanding of the experimental results, computational studies were carried out using the B97D functional with solvent correction using the SMD polarisable continuum in ethanol ($\epsilon = 24.852$). The computational method was first assessed by comparing the optimized geometry of the $[1]^+$ ion with the X-ray crystallographic data in the structure of $[1]^+I^-$.³⁵ As shown in table 4, the theoretical and experimental values are similar, confirming the suitability of the chosen method. Slight differences may be explained by the packing effect on bond distances in the solid state (XRD), whereas the DFT geometry optimization was carried out for an isolated molecule in the polarizable continuum.

Table 4. Comparison of selected experimental and DFT-optimized bond lengths (Å).

				Calculated values
XRD measurement of C-C bond distance in compound [1] ⁺ I ⁻ ^a				Calculated values
	Molecule 1	Molecule 2	Average value	
C1-C2	1.457(8)	1.522(13)	1.490	1.455
C2-C3	1.301(8)	1.346(12)	1.324	1.350
C3-C4	1.487(7)	1.523(12)	1.505	1.491
C4-N	1.492(7)	1.475(9)	1.484	1.552
N-C5	1.503(6)	1.503(6)	1.479	1.505
	1.488(6)	1.470(9)		
	1.482(6)	1.426(9)		

^a Data taken from reference 35.

From a mechanistic point of view, the reaction of a thiolate with the allylic ammonium ion [1]⁺ should involve nucleophilic substitutions via an S_N1, S_N2 or S_N2' mechanism. We have investigated all these pathways (Scheme 3) using methylthiolate as a model nucleophile. The S_N1 mechanism, in which the amine dissociates to yield the carbocation [4]⁺, presents the highest transition state ($\Delta G^\ddagger = 21.9 \text{ kcal mol}^{-1}$), whereas the transition states of the S_N2 ($\Delta G^\ddagger = 15.9 \text{ kcal mol}^{-1}$) and S_N2' ($\Delta G^\ddagger = 18.2 \text{ kcal mol}^{-1}$) pathways are slightly lower. These results indicate that when thiolates are present in the reaction medium, the S_N1 pathway is disfavored. Furthermore, they indicate that the S_N2 pathway is favored relative to the S_N2' pathway, in agreement with the experimental evidence. The free enthalpy difference between the transition states of the two bimolecular pathways, $\Delta(\Delta G^\ddagger) = 2.3 \text{ kcal mol}^{-1}$, corresponds to a rate constant ratio ($k_{\text{S}_{\text{N}2}}/k_{\text{S}_{\text{N}2'}}$) of 24 at 90°C according to the Eyring equation, which translates into a **2:3** ratio of 96/4. This falls within the range of the experimentally observed **2:3** ratios for the various thiolate nucleophiles (table 1, entries 2,3,4,6 and 8).



Scheme 3: Energy diagram for the reaction of methylthiolate MeS^- with ammonium $\mathbf{1}^+$.

Upon taking a closer look at the calculations for the carbocation $\mathbf{[4]}^+$, we note that the $\text{C}_3\text{-C}_4$ bond length is typical (1.35 Å) for a double bond while the $\text{C}_2\text{-C}_3$ bond is longer (1.44 Å), close to the distance expected for a single bond between two sp^2 carbons. The bonding scheme in carbocation $\mathbf{[4]}^+$ (Figure 4) has therefore a large contribution from the Lewis structure given in Figure 4, with the positive charge localized on the C_2 carbon. Moreover, the C_1 , C_2 , C_3 and C_4 atoms are within the same plane, which is bent towards the iron atom, placed at a dihedral angle of 147° relative to the plane of the Cp ring. This bending is provoked by an interaction between C_2 and the electron rich iron atom ($\text{Fe-C}_2 = 2.41 \text{ \AA}$) (see figure 4). A similar distortion has previously been observed by X-ray diffraction analysis of a ferrocenyl carbocation.⁴⁴

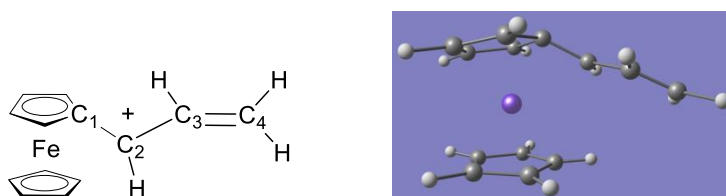
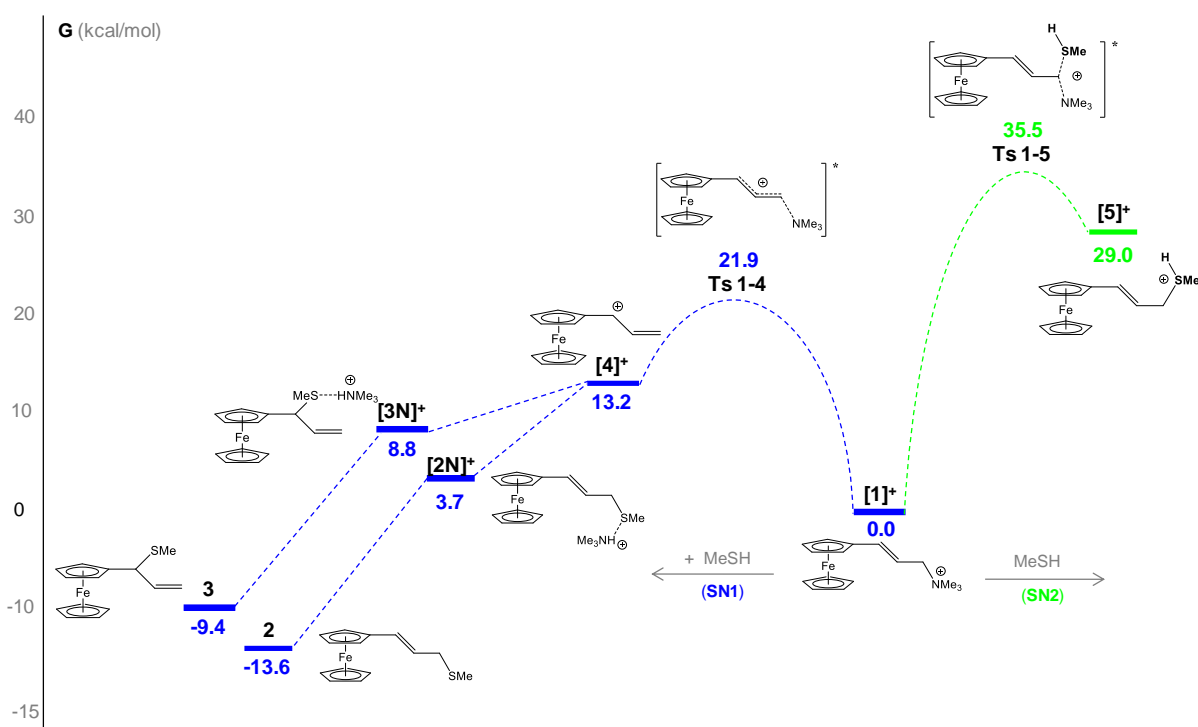


Figure 4. Bonding scheme and DFT optimized structure of carbocation $\mathbf{[4]}^+$.

The computational study of the nucleophilic substitution with the neutral thiols has been realized using methylthiol as model nucleophile. Starting from the allylammonium ion $\mathbf{[1]}^+$,

attack at the carbon bearing the trimethylamine fragment (S_N2) yields a transition state at very high energy ($\Delta G^\ddagger = 35.5 \text{ kcal mol}^{-1}$; Scheme 4), much higher than the S_N2 transition state with methylthiolate. Unfortunately, we were unable to locate the transition state for the S_N2' mechanism. At any rate, this is also likely located at high energy, higher than TS1-4. These results suggest that the nucleophilic substitutions with thiols probably involve an S_N1



Scheme 4: Energy diagram for the reaction of methylthiol MeSH with ammonium $[1]^+$.

The direct addition of thiols to the carbocation $[4]^+$ yields the cationic sulfonium intermediates (see scheme 2). The geometry of the linear isomer $[5]^+$ has been optimized and found to lie at very high energy (29 kcal mol^{-1}) relative to $[1]^+$, whereas the branched isomer $[6]^+$ could not be optimized but is probably also very high in energy. The direct reaction of thiols on carbocation $[4]^+$ is therefore very improbable. The reactions of the H-bonded $\text{MeSH}\cdots\text{NMe}_3$ complex with the substrate $[1]^+$ at both the α and γ C atoms have also been explored, since NMe_3 would be present in solution after the initial formation of the carbocation $[4]^+$ from $[1]^+$. The products of the substitution reactions are the trimethylammonium adducts $[3N]^+$ and $[2N]^+$ (see scheme 4), both found more stable than the free carbocation $[4]^+$. Note also that $[2N]^+$ is much lower in energy than the corresponding sulfonium $[5]^+$ because the very acidic H^+ in $[2N]^+$ has already been transferred to the nitrogen atom of the trimethylamine base, providing strong stabilization. Finally, the free thioethers 2 and 3 are the most stable species.

In this reaction scheme, the two possible sulfonium intermediates, linear **[5]**⁺ and branched **[6]**⁺, are, in fact, never present in the reaction mixture, ruling out the equilibration pathways presented in Scheme 2. This leads us to propose that the reaction regioselectivity (Table 1, entries 1, 5 and 7) corresponds to the regioselectivity of the nucleophile addition to the intermediate carbocation, without further equilibration. Unfortunately, we did not succeed in the optimization of neither the transition states of the processes leading from **[4]**⁺ to **[2N]**⁺ and **[3N]**⁺.

3. Conclusions

We have developed a synthesis of the first ferrocenyl allylic thioethers, obtained in good yields in one step from the ferrocenyallylammonium salt **[1]**⁺I⁻. In the presence of appropriate bases with sufficient strength to generate thiolate anions, interesting level of regioselectivities (88-99%) in favor of the linear isomer were obtained. The mechanistic investigations by DFT calculations have allowed us to propose that a S_N2 mechanism is operative with the thiolate nucleophiles, whereas a dissociative (S_N1) mechanism occurs in the presence of neutral thiols. In the latter case, the proton abstraction from the thiol by trimethylamine is concomitant with the C-S bond formation.

4. Experimental

4.1. General considerations

((2-Ferrocenylvinyl)methyl)trimethylammonium iodide, **[1]**⁺I⁻, was synthesized by a published procedure.³⁵ The different thiols are commercially available and have been used without prior purification (thiophenol from Acros, 99% purity; 2-naphtylthiol from Avocado, 96% purity; 3,5-dimethylthiophenol from Acros, 98% purity; 2-propylthiol from Fluka, 97% purity;. 2-methyl-2-propanethiol from Aldrich, 99% purity). Flash chromatographies were carried out with Silicagel 60A obtained from Carlo Erba. 1D- and 2D-NMR spectra were recorded on a Bruker AV400 spectrometer. ¹H and ¹³C chemical shifts (δ) are given in ppm (the residual peak of the deuterated solvent was used as reference). Peaks are labelled as singlet (s), doublet (d), triplet (t), multiplet (m) and broad (br). The proton and carbon assignments were performed by COSY, HSQC, ¹H-¹³C HMBC experiments. MS spectra were performed by the mass spectrometry service of the Paul Sabatier University, Toulouse.

4.2. General synthesis of thioethers **2** and **3**.

Procedure A: in a Schlenk tube under argon, 103 mg of the salt [1]⁺I⁻ (0.25 mmol) and the desired thiol (2 equiv, 0.50 mmol) were dissolved in 8 ml of *t*BuOH. Procedure B: as above, plus Na₂CO₃ (530 mg, 5.0 mmol, 20 equiv). Procedure C: as for procedure A but with 3 equivalents of thiol (0.75mmol) plus KO^{*t*}Bu (56 mg, 0.5 mmol, 2 equiv). In all cases, the reaction mixture was stirred at 90°C for 16 h. After cooling back to room temperature, the reaction mixture was filtered through filter paper and the purification and product separation were carried out by flash chromatography on silicagel (petroleum ether/ diethyl ether (8/2, v/v) + 1 drop of triethylamine).

Reaction with PhSH

40 mg of **2a** (48%) and 18 mg of **3a** (22%) as yellow solids (procedure A).

60 mg of **2a** (72%) as a yellow solid (procedure B).

(2-ferrocenylvinyl)methyl phenyl sulfide 2a: ¹H (400 MHz, CDCl₃): 7.45-7.42 (2H, m, Ph), 7.36-7.30 (2H, m, Ph), 7.23-7.19 (1H, m, Ph), 6.24 (1H, br d J = 15.6 Hz, CH vinyl), 5.86 (1H, d of t, J = 15.6 Hz, J = 7.2 Hz, CH vinyl), 4.29 (2H, pseudo t, J = 1.9 Hz, subst Cp), 4.19 (2H, pseudo t, J = 1.9 Hz, subst Cp), 4.01 (5H, s, Cp), 3.63 (2H, dd, J = 7.2 Hz, J = 1.3 Hz CH₂). ¹³C (125 MHz, CDCl₃): 136.0 (s, quat. Ph), 130.5 (s, CH vinyl), 129.9 (s, Ph), 128.8 (s, Ph), 126.3 (s, Ph), 122.3 (s, CH vinyl), 82.5 (s, quat. Cp), 69.1 (s, Cp), 68.6 (s, subst. Cp), 66.7 (s, subst. Cp), 37.0 (s, CH₂-vinyl). HR MS (ESI⁺): 334.0476 (100%, 334.0479 for C₁₉H₁₈FeS: M), 225.0366 (54%, 225.0367 for C₁₃H₁₃Fe: M-SPh)

Reaction with 2-naphthylthiol

82 mg of **2b** (85%) as a yellow solid (procedure B).

(2-ferrocenylvinyl)methyl 2-naphthyl sulfide 2b: ¹H (400 MHz, CDCl₃): 7.9-7.7 (4H, m, Ar), 7.55-7.4 (3H, m, Ar), 6.28 (1H, br d J = 15.5 Hz, CH vinyl), 5.90 (1H, d of t, J = 15.5 Hz, J = 7.2 Hz, CH vinyl), 4.28 (2H, pseudo t, J = 1.9Hz, subst Cp), 4.18 (2H, pseudo t, J = 1.9 Hz, subst Cp), 3.95 (5H, s, Cp), 3.74 (2H, dd, J = 7.2 Hz, J = 1.3 Hz CH₂). ¹³C (125 MHz, CDCl₃): 133.7 (s, quat. Ar), 133.6 (s, quat. Ar), 131.9 (s, quat. Ar), 130.7 (s, CH vinyl), 128.3 (s, Ar), 127.9 (s, Ar), 127.8 (s, Ar), 127.1 (s, Ar), 126.5 (s, Ar), 125.7 (s, Ar), 122.0 (s, CH vinyl), 82.5

(s, quat. Cp), 69.1 (s, Cp), 68.6 (s, subst. Cp), 66.7 (s, subst. Cp), 36.9 (s, $\underline{\text{C}}\text{H}_2$ -vinyl). HR MS (ESI+): 384.0636 (100%, 384.0635 for $\text{C}_{23}\text{H}_{20}\text{FeS}$: M), 225.0371 (46%, 225.0367 for $\text{C}_{13}\text{H}_{13}\text{Fe}$: M-SAr).

Reaction with 3,5-dimethylphenylthiol

90 mg of **2c** (66%) as a yellow solid (procedure B).

(2-ferrocenylvinyl)methyl (3,5-dimethylphenyl) sulfide **2c :**

^1H (400 MHz, CDCl_3): 7.05 (2H, s, Ar), 6.85 (1H, s, Ar), 6.25 (1H, t, $J = 15.7$ Hz, CH vinyl), 5.86 (1H, m, CH vinyl), 4.31 (2H, m, subst Cp), 4.20 (2H, m, subst Cp), 4.02 (5H, s, Cp), 3.63 (2H, br d, $J = 7$ Hz, $\underline{\text{C}}\text{H}_2$ -vinyl), 2.33 (6H, s, CH_3). ^{13}C (125 MHz, CDCl_3): 138.4 (s, quat. Ar), 135.6 (s, quat. Ar), 130.3 (s, CH vinyl), 129.0 (s, Ar), 128.2 (s, 2C Ar), 122.3 (s, CH vinyl), 82.6 (s, quat. Cp), 69.2 (s, Cp), 68.6 (s, subst. Cp), 66.7 (s, subst. Cp), 36.8 (s, $\underline{\text{C}}\text{H}_2$ -vinyl), 21.3 (s, 2C $\underline{\text{C}}\text{H}_3$). HR MS (ESI+): 362.0792 (100%, 362.0792 for $\text{C}_{21}\text{H}_{22}\text{FeS}$: M), 225.0372 (40%, 225.0367 for $\text{C}_{13}\text{H}_{13}\text{Fe}$: M-SAr).

Reaction with *i*PrSH

27 mg of **2d** (36%) and 88 mg of **3d** (50%) as yellow solids (procedure B).

67 mg of **2d** (89%) and 3 mg of **3d** (4%) as yellow solids (procedure C).

(2-ferrocenylvinyl)methyl isopropyl sulfide **2d:** ^1H (400 MHz, CDCl_3): 6.21 (1H, br d, $J = 15.5$ Hz, CH vinyl), 5.81 (1H, d of t, $J = 15.5$ Hz, $J = 7.4$ Hz, CH vinyl), 4.34 (2H, pseudo t, $J = 1.9$ Hz, subst Cp), 4.22 (2H, pseudo t, $J = 1.9$ Hz, subst Cp), 4.11 (5H, s, Cp), 3.25 (2H, dd, $J = 7.4$ Hz, $J = 1.3$ Hz $\underline{\text{C}}\text{H}_2$), 2.96 (1H, hept, $J = 6.7$ Hz, CH), 1.32 (6H, d, $J = 6.7$ Hz, CH_3). ^{13}C (125 MHz, CDCl_3): 129.2 (s, CH vinyl), 123.5 (s, CH vinyl), 82.9 (s, quat. Cp), 69.2 (s, Cp), 68.6 (s, subst. Cp), 66.7 (s, subst. Cp), 33.6 (s, CH), 33.5 (s, $\underline{\text{C}}\text{H}_2$ -vinyl), 23.3 (s, CH_3). HR MS (ESI+): 300.0638 (100%, 300.0635 for $\text{C}_{16}\text{H}_{20}\text{FeS}$: M), 225.0373 (19%, 225.0367 for $\text{C}_{13}\text{H}_{13}\text{Fe}$: M-SAr).

(R/S)-(ferrocenyl)(vinyl)methyl isopropyl sulfide **3d:** ^1H (400 MHz, CDCl_3): 6.00 (1H, m, CH vinyl), 5.17-5.08 (2H, m, CH vinyl), 4.26-4.13 (5H, m, 4H subst Cp + 1H $\underline{\text{C}}\text{H}$ -vinyl), 4.21 (5H, s, Cp), 2.86 (1H, m, $\underline{\text{C}}\text{HCH}_3$), 1.31 (3H, d, $J = 6.5$ Hz, CH_3), 1.26 (3H, d, $J = 6.5$ Hz, CH_3). ^{13}C (125 MHz, CDCl_3): 138.6 (s, CH vinyl), 114.1 (s, CH vinyl), 88.0 (s, quat. Cp), 68.8 (s, Cp), 67.9 (s, subst. Cp), 67.6 (s, subst. Cp), 67.5 (s, subst. Cp), 66.5 (s, subst. Cp), 47.1 (s, CH-

vinyl), 34.3 (s, $\underline{\text{C}}\text{HCH}_3$), 23.7 (s, CH_3), 22.9 (s, CH_3) HR MS (ESI⁺): 300.0638 (100%, 300.0635 for $\text{C}_{16}\text{H}_{20}\text{FeS}$: M), 225.0373 (19%, 225.0367 for $\text{C}_{13}\text{H}_{13}\text{Fe}$: M-SAr).

Réaction with *t*BuSH

74 mg (94%) as a 44/56 mixture of **2e** and **3e** (procedure B).

68 mg (87%) as a 84/16 mixture of **2e** and **3e** (procedure B).

HR MS (ESI⁺): 314.0792 (100%, 314.0792 for $\text{C}_{17}\text{H}_{22}\text{FeS}$: M), 225.0369 (26%, 225.0367 for $\text{C}_{13}\text{H}_{13}\text{Fe}$: M-SAr).

(2-ferrocenylvinyl)methyl *tert*-butyl sulfide 2e: ¹H (400 MHz, CDCl_3): 6.28 (1H, d of t, J = 15.5 Hz, J = 1.4 Hz, CH vinyl), 5.85 (1H, d of t, J = 15.5 Hz, J = 7.3 Hz, CH vinyl), 4.33 (2H, pseudo t, J = 1.9 Hz, subst Cp), 4.21 (2H, m, subst Cp), 4.21 (5H, s, Cp), 3.30 (2H, dd, J = 7.3 Hz, J = 1.4 Hz $\underline{\text{C}}\text{H}_2$), 1.404 (9H, s, CH_3). ¹³C (125MHz, CDCl_3): 129.4 (s, CH vinyl), 123.9 (s, CH vinyl), 83.0 (s, quat. Cp), 69.1 (s, Cp), 68.5 (s, subst. Cp), 66.6 (s, subst. Cp), 31.8 (s, $\underline{\text{C}}\text{H}_2$), 31.6 (s, $\underline{\text{C}}\text{CH}_3$), 31.1 (s, CH_3).

(R/S)-(ferrocenyl)(vinyl)methyl *tert*-butyl sulfide 3e: ¹H (400 MHz, CDCl_3): 6.16 (1H, m, CH vinyl), 5.23 (1H, br d, J = 17.0 Hz, CH vinyl), 5.16 (1H, br d, J = 10.0 Hz, CH vinyl), 4.3-4.1 (5H, m, 4H subst Cp + 1H CH), 4.21 (5H, s, Cp), 1.395 (9H, s, CH_3). ¹³C (125 MHz, CDCl_3): 141.4 (s, CH vinyl), 114.0 (s, CH vinyl), 89.6 (s, quat. Cp), 68.8 (s, Cp), 67.9 (s, subst. Cp), 67.64 (s, subst. Cp), 67.61 (s, subst. Cp), 67.0 (s, subst. Cp), 45.8 (s, CH), 31.6 (s, $\underline{\text{C}}\text{CH}_3$), 31.1 (s, CH_3).

4.3. X-ray structural analyses of 2a and 2b

A single crystal of each compound was mounted under inert perfluoropolyether at the tip of a glass fibre and cooled in the cryostream of a Rigaku Oxford-Diffraction GEMINI EOS diffractometer.

The structures were solved by direct methods (SIR97⁴⁵) and refined by least-squares procedures on F^2 using SHELXL-97.⁴⁶ All H atoms attached to carbon were introduced in calculated positions and treated as riding models. The absolute structure for compounds **2a** has been evaluated by refining the Flack's parameter.⁴⁷ The drawing of the molecules was realised with the help of ORTEP32.^{48,49} Crystal data and refinement parameters are shown in Table 4.

Table 4: Crystal Data

Identification code	2a	2b
Empirical formula	C ₃₈ H ₃₆ Fe ₂ S ₂	C ₂₃ H ₂₀ FeS
Formula weight	668.49	384.30
Temperature, K	173(2)	173(2)
Wavelength, Å	0.71073	0.71073
Crystal system	Orthorhombic	Monoclinic
Space group	Fdd2	P2 ₁ /c
a, Å	51.2494(10)	5.8000(2)
b, Å	40.5129(9)	14.9194(4)
c, Å	5.94660(10)	20.6292(5)
α, °	90.0	90.0
β, °	90.0	91.410(2)
γ, °	90.0	90.0
Volume, Å ³	12346.7(4)	1784.56(9)
Z	16	4
Density (calc), Mg/m ³	1.439	1.430
Abs. coefficient, mm ⁻¹	1.102	0.964
F(000)	5568	800
Crystal size, mm ³	0.370 x 0.130 x 0.130	0.180 x 0.100 x 0.050
Theta range, °	3.120 to 26.369	2.904 to 26.372
Reflections collected	30927	18623
Indpt reflections (R _{int})	5981 (0.026)	3643 (0.0314)
Completeness, %	99.7	99.6
Absorption correction	Multi-scan	Multi-scan
Max. / min. transmission	1.0 / 0.914	1.0 and 0.944
Refinement method	F ²	F ²
Data /restraints/parameters	5981 / 1 / 379	3643 / 0 / 226
Goodness-of-fit on F ²	1.044	1.028
R1, wR2 [I>2σ(I)]	0.0210, 0.0469	0.0315, 0.0717
R1, wR2 (all data)	0.0231, 0.0477	0.0389, 0.0751
Flack's parameter	-0.012(4)	
Residual density, e.Å ⁻³	0.188 / -0.169	0.934 / -0.285

Crystallographic data for compounds **2a** and **2b** (excluding structure factors) have been deposited with the Cambridge Crystallographic Data Centre as supplementary publication no. CCDC 1542978-1542979. Copies of the data can be obtained free of charge on application to the Director, CCDC, 12 Union Road, Cambridge CB2 1EZ, UK (fax: (+44) 1223-336-033; e-mail: deposit@ccdc.cam.ac.uk).

Computational Details. The calculations were carried out within the DFT approach with the B97D functional, including an ultrafine integration grid, as implemented in Gaussian 09. All geometry optimizations were carried out using the SDD basis set and ECP for the Fe atom, augmented with an f polarization function ($\alpha = 2,462$),⁵⁰ and the 6-31G(d,p) basis sets for all other atoms. The effect of the solvent was included by the SMD polarisable continuum⁵¹ in ethanol ($\epsilon = 24.852$) during the geometry optimizations. All of the energies presented in the text are Gibbs energies in ethanol (ΔG_{EtOH}).

Acknowledgements

We thank the Centre National de la Recherche Scientifique (CNRS) for support. RB thanks the “Ministère de l’Enseignement Supérieur et la Recherche Scientifique” of Algeria for generous funding of her Internship in Toulouse. This work was granted access to the HPC resources of IDRIS under the allocation 2016-086343 made by GENCI (Grand Equipement National de Calcul Intensif) and to the resources of the CICT (Centre Interuniversitaire de Calcul de Toulouse, project CALMIP).

References

-
- ¹ Y. Yatsumonji, Y. Ishida, A. Tsubouchi, T. Takeda *Org. Lett.*, **2007**, *9*, 4603-4606.
 - ² A. B. Zaitsev, H. F. Caldwell, P. S. Pregosin, L. F. Veiros *Chem. Eur. J.*, **2009**, *15*, 6468 – 6477.
 - ³ S. Tanaka, P. K. Pradhan, Y. Maegawa, M. Kitamura *Chem. Commun.*, **2010**, *46*, 3996–3998.
 - ⁴ F. Robertson, J. Wu *Org. Lett.*, **2010**, *12*, 2668-2671.
 - ⁵ N. Gao, S. Zheng, W. Yang, X. Zhao *Org. Lett.*, **2011**, *13*, 1514-1516.
 - ⁶ J. A. van Rijn, M. C. Guijt, D. de Vries, E. Bouwman, E. Drent *Appl. Organometal. Chem.* **2011**, *25*, 212–219.

-
- ⁷ M. Roggen, Erick M. Carreira *Angew. Chem. Int. Ed.* **2012**, *51*, 8652–8655.
- ⁸ V. Pace, L. Castoldi, W. Holzer *Tet.Lett.*, **2012**, *53*, 967–972.
- ⁹ S. Banerjee, L. Adak, B. C. Ranu *Tet. Lett.*, **2012**, *53*, 2149–2153.
- ¹⁰ P. N. Chatterjee, S. Roy *Tetrahedron*, **2012**, *68*, 3776–3785.
- ¹¹ L. Herkert, S. L. J. Green, G. Barker, D. G. Johnson, P. C. Young, S. A. Macgregor, A.-L. Lee *Chem. Eur. J.*, **2014**, *20*, 11540–11548.
- ¹² G. Tabarelli, M. Godoi, R. F. S. Canto, J. R. Mora, F. Nome, A. L. Braga *Synth. Commun.*, **2014**, *44*, 3441–3449.
- ¹³ A. B. Pritzius, B. Breit *Angew. Chem. Int. Ed.*, **2015**, *54*, 3121–3125.
- ¹⁴ B. B. Aggarwal, S. Shishodia *Biochem. Pharmacology*, **2006**, *71*, 1397–1421.
- ¹⁵ (b) L. Brunsveld, J. Kuhlmann, K. Alexandrov, A. Wittinghofer, R. S. Goody, H. Waldmann *Angew. Chem. Int. Ed.*, **2006**, *45*, 6622–6646.
- ¹⁶ J. He, M. Zha, J. Cui, M. Zeller, A. D. Hunter, S.-M. Yiu, S.-T. Lee, Z. Xu *J. Am. Chem. Soc.*, **2013**, *135*, 7807–7810.
- ¹⁷ R. Malherbe, G. Rist, D. Bellus *J. Org. Chem.*, **1983**, *48*, 860–869.
- ¹⁸ E. Vedejs *Acc. Chem. Res.*, **1984**, *135*, 7807–7810.
- ¹⁹ R. Oehrlein, R. Jeschke, B. Ernst, D. Bellus *Tet. Lett.*, **1989**, *30*, 3517–3520.
- ²⁰ S. Barluenga, P. Lopez, E. Moulin, N. Winssinger *Angew. Chem. Int. Ed.*, **2004**, *43*, 3467–3470.
- ²¹ D. Crich, Y. Zou, F. Brebion *J. Org. Chem.*, **2006**, *71*, 9172–9177.
- ²² Y. A. Lin, J. M. Chalker, N. Floyd, G. J. L. Bernardes, B. G. Davis *J. Am. Chem. Soc.*, **2008**, *130*, 358–364.
- ²³ T. J. Colacot *Chem. Rev.* **2003**, *103*, 3101–3118.
- ²⁴ R. C. J. Atkinson, V. C. Gibson, N. J. Long *Chem. Soc. Rev.* **2004**, *33*, 313–328.
- ²⁵ R. Gomez Arrayas, J. Adrio, J. C. Carretero, *Angew. Chem. Int. Ed.* **2006**, *68*, 3679.
- ²⁶ A. Fihri, P. Meunier, J.-C. Hierso *Coord. Chem. Rev.* **2007**, *251*, 2017–2055.
- ²⁷ W. Chen, H.-U. Blaser, “Ligands with planar chirality: planar chiral ferrocene- and paracyclophane-based diphosphines” ed. by A. Börner (Wiley-VCH, Weinheim, Germany), **2008** 345–359.
- ²⁸ P. Stepnicka, M. Lamac, “Synthesis and catalytic use of planar chiral and polydentate ferrocene donors” ed. by P. Stepnicka (John Wiley, Chichester, UK), **2008**, 345–359.
- ²⁹ E. Manoury, R. Poli, “Phosphine-Containing Planar Chiral ferrocenes: Synthesis, Coordination Chemistry and Applications to Asymmetric Catalysis.” in the Series: Catalysis by Metal Complexes (CMCO), Volume 36 (Phosphorus Chemistry: Catalysis and Material Science Applications), ed. by M. Peruzzini and L. Gonsalvi (Springer Verlag, Germany), **2011**, 121–149.
- ³⁰ S. Toma, J. Csizmadiova, M. Meciarova, R. Sebesta *Dalton Trans.*, **2014**, *43*, 16557–16579.
- ³¹ R. Sun, L. Wang, H. Yu, Z. Abdin, Y. Chen, J. Huang, R. Tong *Organometallics*, **2014**, *33*, 4560–4573.
- ³² L. Peng, A. Feng, M. Huo, J. Yuan *Chem. Commun.*, **2014**, *50*, 13005–13014.
- ³³ S. S. Braga, A. M. S. Silva *Organometallics*, **2013**, *32*, 5626–5639.
- ³⁴ V. N. Babin, Yu. A. Belousov, V. I. Borisov, V. V. Gumenyuk, Yu. S. Nekrasov, L. A. Ostrovskaya, I. K. Sviridova, N. S. Sergeeva, A. A. Simenel, L. V. Snegur *Russ. Chem. Bull., Int. Ed.*, **2014**, *63*, 2405–2422.
- ³⁵ R. Bouchene, J.-C. Daran, S. Bouacida, E. Manoury, *Eur. J. Inorg. Chem.*, **2017**, 340–350.
- ³⁶ G. A. Olah, D. H. O’Brien, C. U. Pittmann, Jr, *J. Am. Chem.*, **1967**, *89*, 2996–3001.
- ³⁷ P. Bonvicini, A. Levi, V. Lucchini, G. Scorrano, *J. Chem. Soc. Perkin II*, **1972**, 2267–2269.

-
- ³⁸ M. Eckert-Maksic, R. Boscovic, *J. Chem.Soc. Perkin II*, **1981**, 62-64.
- ³⁹ P. Traldi, *J. Heterocyclic Chem.*, **1989**, 26, 465-468.
- ⁴⁰ For the pKa of thiol/thiolate couples, see: B. Thapa, H. B. Schlegel, *J. Phys.. Chem. A*, **2016**, 120, 5726-5735 and references herein.
- ⁴¹ M. B. Smith and J. March, *March's Advanced Organic Chemistry: Reactions, Mechanisms, and Structure 6th edn* (John Wiley & Sons, Hoboken, NJ), **2007**, 469-473.
- ⁴² S. Zhang, *J. Comput.. Chem.*, **2011**, 33, 517-526.
- ⁴³ A. L. Spek, *J. Appl. Cryst.*, **2003**, 36, 7-13.
- ⁴⁴ A. Z. Kreidlin, F. M. Dolgushin, A. I. Yanovsky, Z. A. Kerzina, P. V. Petrovskii, *J. Organomet. Chem.* **2000**, 616, 106-111.
- ⁴⁵ A. Altomare, M. C. Burla, M. Camalli, G. L. Casciarano, C. Giacovazzo, A. Guagliardi, A. G. Moliterni, G. Polidori, R. Spagna, *SIR97- a program for automatic solution of crystal structures by direct methods. J. Appl. Cryst.*, **1999**, 32, 115-119.
- ⁴⁶ G. M. Sheldrick, *Acta Cryst.*, **2008**, A64, 112-122.
- ⁴⁷ H. D. Flack, *Acta Cryst.* , **1983**, A39, 876-881.
- ⁴⁸ L. J. Farrugia, "ORTEP-3 for Windows", *J. Appl. Cryst.*, **1997**, 30, 565.
- ⁴⁹ M. N. Burnett, C. K. Johnson, "ORTEPIII" *Report ORNL-6895*, **1996**, Oak Ridge National Laboratory, Tennessee, USA
- ⁵⁰ A. W. Ehlers, M. Boehme, S. Dapprich, A. Gobbi, A. Hoellwarth, V. Jonas, K. F. Koehler, R. Stegmann, A. Veldkamp, G. Frenking, *Chem. Phys. Lett.*, **1993**, 208, 111-114.
- ⁵¹ A. V. Marenich, C. J. Cramer, D. G. Truhlar, *J. Phys. Chem. B*, **2009**, 113, 6378-6396.